Available online at www.sciencedirect.com
SCIENCE DIRECT
Bioorganic & Medicinal Chemistry
Bioorganic & Medicinal Chemistry 14 (2006) 3872–3882

# Binding of oxalyl derivatives of β-D-glucopyranosylamine to muscle glycogen phosphorylase b

Theodoros Hadjiloi,[a,†] Costas Tiraidis,[a] Evangelia D. Chrysina,[a] Demetres D. Leonidas,[a] Nikos G. Oikonomakos,[a,b,*] Panagiotis Tsipos[c] and Thanasis Gimisis[c]

[a]*Institute of Organic and Pharmaceutical Chemistry, The National Hellenic Research Foundation, 48 Vas. Constantinou Ave., 116 35 Athens, Greece*
[b]*Institute of Biological Research and Biotechnology, The National Hellenic Research Foundation, 48 Vas. Constantinou Ave., 116 35 Athens, Greece*
[c]*Organic Chemistry Laboratory, Department of Chemistry, University of Athens, Panepistimiopolis, 15771 Athens, Greece*

Received 2 December 2005; revised 13 January 2006; accepted 17 January 2006
Available online 7 February 2006

**Abstract**—Five oxalyl derivatives of β-D-glucopyranosylamine were synthesized as potential inhibitors of glycogen phosphorylase (GP). The compounds **1**–**4** were competitive inhibitors of rabbit muscle GPb (with respect to α-D-glucose-1-phosphate) with $K_i$ values of 0.2–1.4 mM, while compound **5** was not effective up to a concentration of 10 mM. In order to elucidate the structural basis of their inhibition, we analysed the structures of compounds **1**–**4** in complex with GPb at 1.93–1.96 Å resolution. The complex structures reveal that the inhibitors can be accommodated at the catalytic site at approximately the same position as α-D-glucose and stabilize the T-state conformation of the 280s loop by making several favourable contacts to Asp283 and Asn284 of this loop. Comparison with the lead compound *N*-acetyl-β-D-glucopyranosylamine (**6**) shows that the hydrogen bonding interaction of the amide nitrogen with the main-chain carbonyl oxygen of His377 is not present in these complexes. The differences observed in the $K_i$ values of the four analogues can be interpreted in terms of subtle conformational changes of protein residues and shifts of water molecules in the vicinity of the catalytic site, variations in van der Waals interactions, conformational entropy and desolvation effects.


## 1. Introduction

Understanding the fundamental mechanisms that regulate glycogen metabolism provides a basis for therapy of type 2 diabetes. High blood glucose concentration in type 2 diabetes is, in part, due to abnormal production of glucose by the liver. Glycogen is an important source of hepatic glucose production, therefore, inhibition of hepatic glycogen phosphorylase (GP), which catalyses the first step in glycogen breakdown, is a potential therapeutic strategy.[1–5] GP inhibitors may bind predominantly to four distinct sites, the catalytic, the allosteric, the indole carboxamide and the inhibitor or caffeine site,[6–14] while a new binding site capable of accommodating benzimidazole has been recently discovered.[15] Recently, the synthesis and in vitro and in vivo biological evaluation of corosolic acid and maslinic acid derivatives, inhibitors of GP, have been reported;[42,43] furthermore, FR258900, a novel GP inhibitor, isolated from fungal strain No. 138354, was shown to stimulate glycogen synthesis in primary hepatocytes via GP inhibition.[44,45] The efficacy of such inhibitors on control of blood glucose and hepatic glycogen balance has been confirmed from animal studies and in vitro cell biology experiments.[3,16]

The catalytic site of GP has been extensively exploited for development of potent inhibitors of the enzyme.[15,17–31] Sometime ago *N*-acetyl-β-D-glucopyranosylamine (**6**)

*Abbreviations*: GP, glycogen phosphorylase; 1,4-α-D-Glucan:orthophosphate α-glucosyltransferase (EC 2.4.1.1); GPb, rabbit muscle glycogen phosphorylase b; PLP, pyridoxal 5′-phosphate; Glucose, α-D-glucose; Glc-1-P, α-D-glucose 1-phosphate; Compound **1**, *N*-(β-D-glucopyranosyl)oxamic acid; Compound **2**, methyl *N*-(β-D-glucopyranosyl)oxamate; Compound **3**, ethyl *N*-(β-D-glucopyranosyl)oxamate; Compound **4**, *N*-(β-D-glucopyranosyl)-*N*′-cyclopropyl oxalamide; Compound **5**, *N*-(β-D-glucopyranosyl)-*N*′,*N*′-diisopropyl oxalamide; Rms deviation, root-mean-square deviation.

*Keywords*: Type 2 diabetes; Glycogen phosphorylase; Oxalyl derivatives; Inhibition; X-ray crystallography.

* Corresponding author. Tel.: +30 210 7273761; fax: +30 210 7273831; e-mail: ngo@eie.gr
† Present address: CERM, Via Sacconi, 6, 50019 Sesto Fiorentino (FI), Italy.

0968-0896/$ - see front matter © 2006 Elsevier Ltd. All rights reserved.
doi:10.1016/j.bmc.2006.01.045

was found to be a potent inhibitor of muscle GPb with a $K_i = 32\ \mu M$.[20] Structural information available from the crystal structure of the inhibitor complex at 2.3 Å[20] and recently at 1.9 Å resolution[31] showed that **6**, on binding to GPb, promotes the less active T state enzyme through stabilization of the closed position of 280 s loop (residues 282–287), which blocks access of the substrate to the catalytic site. The inhibitor fits tightly into the so-called β-pocket, a side channel from the catalytic site with no access to the bulk solvent.[17] In addition, there is a hydrogen bond between N1 of **6** and carbonyl O of His377, an interaction that since then has been observed in all β-D-glucopyranosylamine and spirohydantoin analogues of β-D-glucopyranose.[15,21,26,29,30] Identification of the structural determinants contributing to inhibitor binding mode at the catalytic site should provide a better understanding of the mechanism of inhibition of GP and aid in the design of compounds with improved potency against GP.

A novel class of oxalyl derivatives of β-D-glucopyranosylamine (**1**–**5**, Scheme 1) were identified as competitive inhibitors of GPb with $K_i$ values 0.2–1.4 mM. We report here on the crystallographic binding of derivatives **1**–**4** to GPb, in order to provide rationalizations for the kinetic properties of the compounds. The crystallographic data show that the compounds bind at the catalytic site and occupy a position similar but not identical to that of the lead compound **6**. On binding of **1**–**4** to the enzyme there are subtle changes of the amino acid side chains and water structure in the vicinity of the catalytic site, while the characteristic hydrogen bond between the

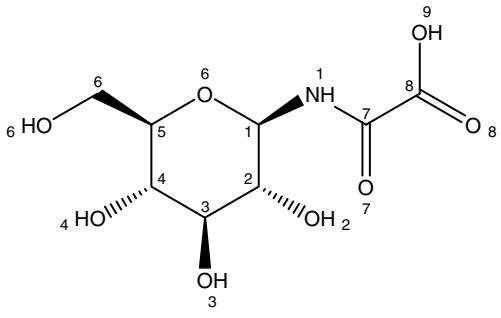

**1** ($K_i$=0.71 mM)

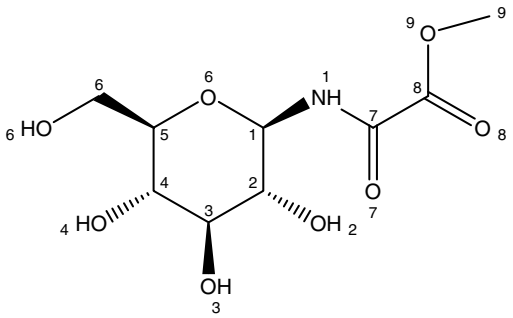

**2** ($K_i$=0.21 mM)

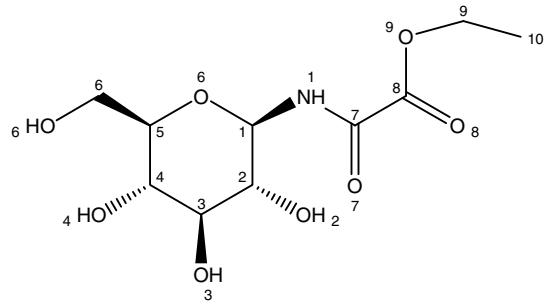

**3** ($K_i$=0.92 mM)

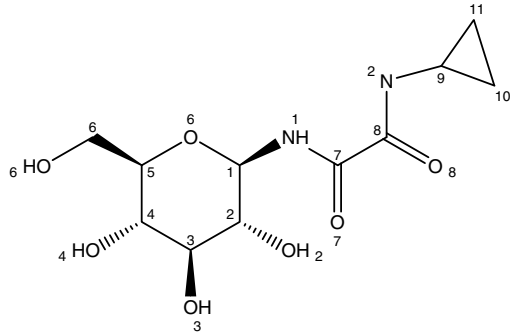

**4** ($K_i$=1.41 mM)

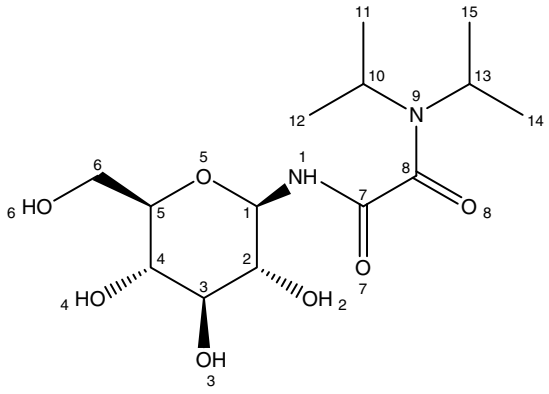

**5** (No inhibition)

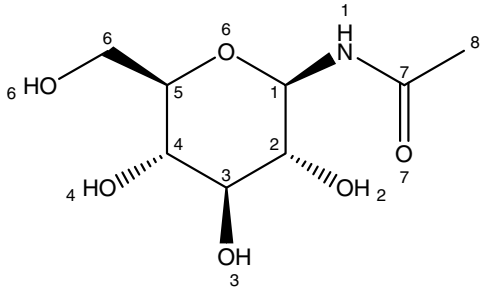

**6** ($K_i$=0.032 mM)

**Scheme 1.** Chemical structures of oxalyl derivatives of β-D-glucopyranosylamine (**1**–**5**) and *N*-acetyl-β-D-glucopyranosylamine (**6**), showing the numbering system used.

**Table 1.** Summary of diffraction data and refinement statistics for GPb: **1**–**4** complexes

| Compound | **1** | **2** | **3** | **4** |
|---|---|---|---|---|
| Space group | $P4_32_12$ | $P4_32_12$ | $P4_32_12$ | $P4_32_12$ |
| No. of images (°) | 80 (56°) | 91 (63.7°) | 83 (51.6°) | 81 (56.7°) |
| Unit cell dimensions (Å) | $a = b = 128.0$, $c = 115.7$ | $a = b = 128.6$, $c = 116.1$ | $a = b = 128.3$, $c = 116.0$ | $a = b = 128.0$, $c = 116.0$ |
| Resolution range (Å) | 30.0–1.94 | 30.0–1.96 | 30.0–1.96 | 30.0–1.93 |
| No. of observations | 412,739 | 623,378 | 478,394 | 532,292 |
| No. of unique reflections | 71,101 (3500) | 70286 (3459) | 68828 (3392) | 72265 (3554) |
| Outermost shell (Å) | 1.97–1.94 | 1.99–1.96 | 1.99–1.96 | 1.96–1.93 |
| Multiplicity (outermost shell) | 4.4 (4.2) | 5.3 (5.3) | 4.2 (4.2) | 4.0 (4.0) |
| $\langle I/\sigma(I)\rangle$ (outermost shell) | 10.7 (2.2) | 15.3 (4.5) | 20.6 (3.8) | 6.6 (1.9) |
| Completeness (outermost shell) (%) | 99.6 (99.5) | 99.6 (99.6) | 98.5 (98.1) | 99.3 (99.1) |
| $R_m$ (outermost shell) | 0.055 (0.415) | 0.067 (0.516) | 0.042 (0.443) | 0.059 (0.380) |
| *B*-values (Å$^2$) (Wilson plot) | 22.6 | 26.3 | 28.2 | 27.9 |
| Refinement (resolution) (Å) | 30.0–1.94 | 30.0–1.96 | 30.0–1.96 | 30.0–1.93 |
| No. of reflections used (free) | 67,468 (3608) | 66,329 (3,555) | 65,294 (3501) | 68,490 (3668) |
| Residues included | (12–254), (261–314), (324–836) | (12–254), (261–314), (324–836) | (12–254), (261–314), (324–836) | (12–254), (261–314), (324–836) |
| No. of protein atoms | 6590 | 6590 | 6590 | 6590 |
| No. of water molecules | 351 | 315 | 317 | 300 |
| No. of ligand atoms | 15 (PLP), 17 (**1**) | 15 (PLP), 18 (**2**) | 15 (PLP), 19 (**3**) | 15 (PLP), 20 (**4**) |
| Final *R* ($R_{free}$) (%) | 19.3 (21.8) | 18.3 (19.9) | 18.5 (21.3) | 19.1 (21.1) |
| *R* ($R_{free}$), outermost shell (%) | 26.7 (29.2) | 23.4 (27.1) | 24.7 (27.2) | 26.1 (26.5) |
| RMSD in bond lengths (Å) | 0.006 | 0.005 | 0.005 | 0.005 |
| RMSD in bond angles (°) | 1.25 | 1.20 | 1.21 | 1.24 |
| RMSD in dihedrals (°) | 21.9 | 21.4 | 21.7 | 25.2 |
| RMSD in impropers (°) | 0.78 | 0.76 | 0.81 | 0.69 |
| Average *B* (Å$^2$) for residues | (12–254), (261–314), (324–836) | (12–254), (261–314), (324–836) | (12–254), (261–314), (324–836) | (12–254), (261–314), (324–836) |
| Overall | 29.5 | 31.1 | 33.7 | 34.2 |
| Cα, C, N, O | 27.4 | 28.9 | 31.4 | 32.0 |
| Side chain | 31.5 | 33.3 | 35.9 | 36.3 |
| Average *B* (Å$^2$) for heteroatoms | 17.5 (PLP), 21.7 (**1**) | 19.0 (PLP), 25.1 (**2**) | 20.7 (PLP), 27.5 (**3**) | 21.6 (PLP), 29.7 (**4**) |
| Average *B* (Å$^2$) for water molecules | 37.7 | 37.9 | 36.9 | 40.9 |

Merging $R_m$ is defined as $R_m = \Sigma_i \Sigma_h|\langle I_h\rangle - I_{ih}|/\Sigma_i\Sigma_h I_{ih}$, where $\langle I_h\rangle$ and $I_{ih}$ are the mean and *i*th measurement of intensity for reflection *h*, respectively. $\sigma(I)$ is the standard deviation of *I*. Crystallographic *R* factor is defined as $R = \Sigma||F_o| - |F_c||/\Sigma|F_o|$, where $|F_o|$ and $|F_c|$ are the observed and calculated structure factor amplitudes, respectively. $R_{free}$ is the corresponding *R* value for a randomly chosen 5% of the reflections that were not included in the refinement.

amide nitrogen N1 and main-chain O of His377 is not present in the crystal complex structures studied.

## 2. Materials and methods

The syntheses of compounds **1**–**5** and their kinetic experiments with rabbit muscle GPb will be described elsewhere (Gimisis et al., unpublished results). GPb was isolated, purified, recrystallized and assayed as described.[25] Native GPb crystals, grown in the tetragonal lattice[32] spacegroup $P4_32_12$, were soaked with 100 mM compound **1** (for 48 h) or 20 mM of **2** (for 6 h) or 25 mM **3** (for 48 h) or 10 mM of **4** (for 24 h) or 50 mM of **5** (for 5 h) in a buffered solution (10 mM Bes, 0.1 mM EDTA and 0.02% sodium azide, pH 6.7), prior to data collection. Diffraction data were collected from single crystals at Daresbury Laboratory (Station 9.6) and EMBL-Hamburg outstation (Beamlines X11 and X13) to a resolution of 1.93–1.96 Å. The reflections were recorded on an ADSC Q4 CCD detector. Data reduction and integration followed by scaling and merging of the intensities obtained were performed with Denzo and Scalepack, respectively, as implemented in HKL suite.[33]

Crystallographic refinement of the four complexes was performed with CNS version 1.1[34] using positional and individual B-factor refinement with bulk-solvent correction. The starting model employed for the refinement of the complexes was the structure of the GPb-α-D-glucose complex determined at 2.1 Å resolution (Oikonomakos et al., unpubl.). $2F_o - F_c$ and $F_o - F_c$ electron density maps calculated were visualized using the program for molecular graphics 'O.'[35] Ligand models, constructed and minimized using the program SYBYL (Tripos Associates Inc. 1992 SYBYL Molecular Modelling Software, St. Louis, Missouri, USA), were fitted to the electron density maps after adjustment of their torsion angles. Alternate cycles of manual rebuilding with 'O' and refinement with CNS improved the quality of the models. The data collection and refinement statistics are summarized in Table 1.

The stereochemistry of the protein residues was validated by PROCHECK.[36,37] Hydrogen bonds and van der Waals interactions were calculated with the program CONTACT as implemented in CCP4 (CCP4, 1994) applying a distance cut-off of 3.3 and 4.0 Å, respectively. The program calculates the angle O···H···N (where the hydrogen position is unambiguous) and the angle source . . .oxygen-bonded carbon atom. Suitable values are 120° and 90°. A Luzatti plot[38] suggests an average positional error for all structures of approximately 0.24–0.26 Å. GPb complex structures were superimposed over well-defined residues using LSQKAB.[37] Comparisons of the water molecules in the complex structures were made taking into consideration their equivalent positions. The schematic representation of the crystal structures presented in all figures were prepared with the programs MolScript[39] and BobScript[40] and rendered with Raster3D.[41] The coordinates of the new structures have been deposited with the RCSB Protein Data Bank (http://www.rcsb.org/pdb) with codes 2F3P (GPb-**1** complex), 2F3Q (GPb-**2** complex), 2F3S (GPb-**3** complex), and 2F3U (GPb-**4** complex).

## 3. Results and discussion

The kinetic parameters of compounds **1**–**5**, assayed with GPb into the direction of glycogen synthesis (Gimisis et al., unpublished results), are summarized in Scheme 1. Compound **2** was found to be a better inhibitor ($K_i = 0.22 \pm 0.01$ mM) than **1** ($K_i = 0.71 \pm 0.02$ mM) or **3** ($K_i = 0.92 \pm 0.05$ mM) or **4** ($K_i = 1.41 \pm 0.09$ mM). The kinetic results showed also that compound **5** is not an inhibitor when tested up to a concentration of 10 mM.

In order to elucidate the structural basis of inhibition we have determined the crystal structure of GPb in complex with **1**–**4**. A summary of the data processing and refinement statistics for the **1**–**4** complex structures is given in Table 1. The resulting electron density map for compound **5** showed poor binding to the catalytic site, in agreement with the kinetic results, and indicated that the *N*′,*N*′-diisopropyl oxalamide group had displaced Asp283 and Asp284 of the 280s loop. The refinement

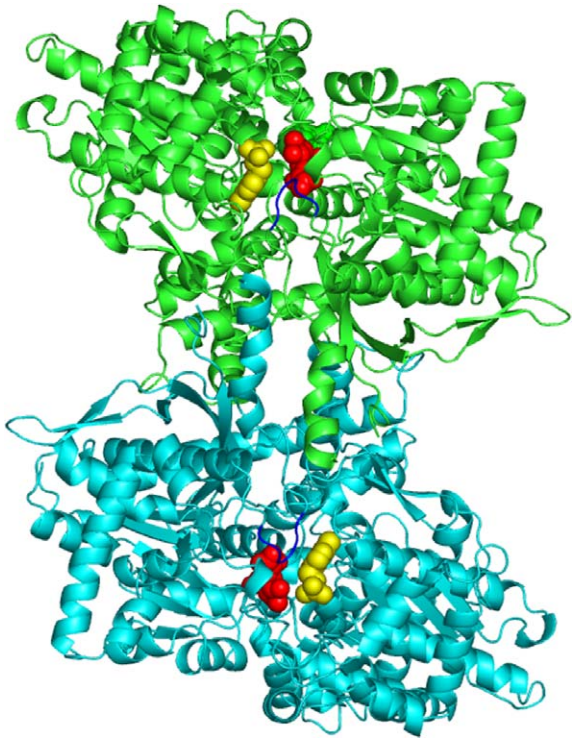

**Figure 1.** A schematic diagram of the GPb dimeric molecule viewed down the molecular dyad. One subunit is coloured in green and the other in cyan. The position is shown for the catalytic site. The catalytic site, marked by *N*-(β-D-glucopyranosyl)oxamic acid (compound **1**, in red) and the essential cofactor pyridoxal 5′-phosphate (in yellow), shown in ball-and-stick representations, is buried at the centre of the subunit and is accessible to the bulk solvent through a 15-Å long channel. Compound **1**, on binding at the catalytic site, promotes the less active T state through stabilisation of the closed position of the 280s loop (shown in blue) which blocks access for the substrate (glycogen) to the catalytic site.

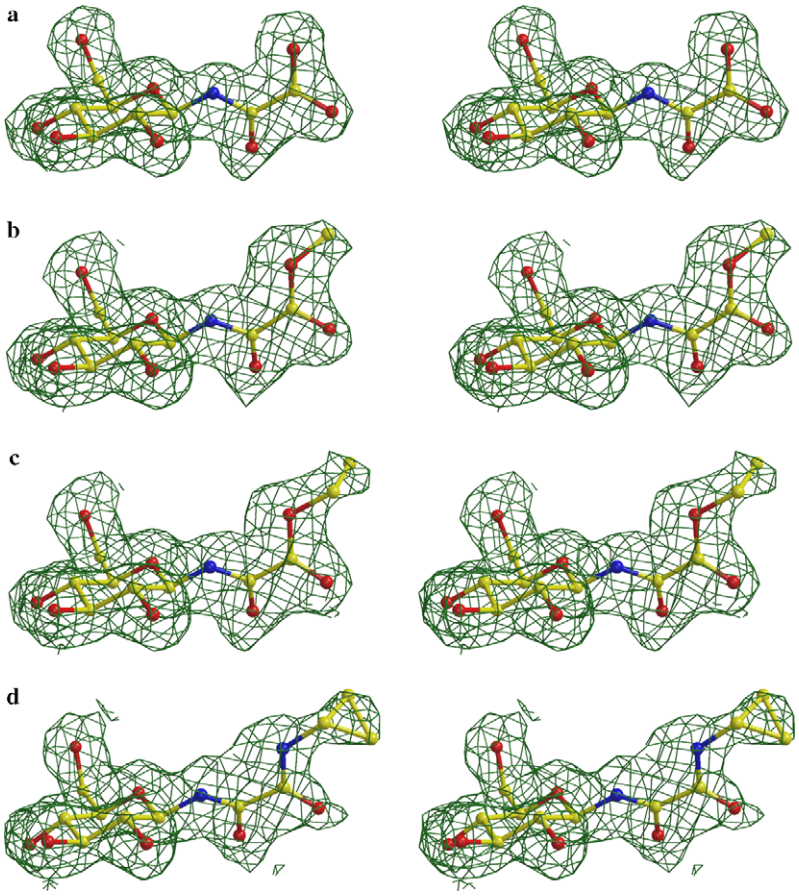


**Figure 2.** Stereo diagrams of the $2F_o - F_c$ electron density maps, contoured at $1\sigma$, for the bound compounds **1** (a), **2** (b), **3** (c) and **4** (d) at the catalytic site. Electron density maps were calculated using the standard protocol as implements in CNS v1.1[34] before incorporating ligand coordinates.

for this complex was terminated in view of the negative result. For the **1**–**4** complexes, the $2F_o - F_c$ Fourier electron density maps indicated that compounds **1**–**4** bound at the catalytic site (Fig. 1). Electron density maps (Fig. 2) clearly defined the position of each inhibitor within the catalytic site, consistent with the kinetic results. We describe in detail the GPb:**1** interactions and briefly the GPb:**2**–**4** interactions at the catalytic site.

### 3.1. Compound 1

The mode of binding and the interactions that the glucopyranose moiety of **1** make with GPb are almost identical with those for α-D-glucose.[17] The oxamic acid group can be accommodated at the β-pocket of the catalytic site and stabilises the closed conformation of the 280s loop. Thus, O7 makes a hydrogen bonding interaction with Asp283 OD1 through Wat349; O8 makes a direct hydrogen bond with Asn284 N, a water-mediated hydrogen bond with Asp283 OD1, and also it exploits an extended hydrogen bonding pattern between Wat349 and Gly134 N, Gly137 N and Glu88 OE2 through another water molecule (Wat79); O9 is hydrogen bonded with His341 NE2 through Wat351 (Table 2). The hydrogen bonds formed between the ligand and the protein are illustrated in Figure 3a.

Compound **1**, on binding to GPb, makes a total of 17 hydrogen bonds and 88 van der Waals interactions (7 nonpolar/nonpolar, 21 polar/polar and 60 polar/nonpolar) (Table 3). It is a moderate inhibitor ($K_i$ = 0.71 mM) and binds almost 2.5 times more tightly than α-D-glucose ($K_i$ = 1.7 mM) or 10 times more tightly than its parent compound β-D-glucose ($K_i$ = 7.4 mM),[17] possibly because of the additional interactions of the oxamic acid group with the protein.

Compound **1** appears to form an improved network of interactions compared to the lead molecule **6** (Fig. 3e), however it exhibits poorer affinity than **6**. A structural comparison between the GPb-**1** complex and the GPb-**6** complex shows that the positions of Cα for residues 18–249, 262–312, and 326–829 deviate from their mean positions by 0.107 Å, indicating overall negligible changes between the complex structures. However, comparison reveals a conformational shift for Asp339; the dihedral angle χ2 [CA-CB-CG-OD1] is rotated by 90° in order to avoid close contacts with O9 of the oxamic acid group of **1**. There are also small shifts of the side chain atoms of Leu136 and Asp283; thus, on ligand binding, the side chains of Leu136 and Asp283 are rotated by ~90° and ~12°, respectively (dihedral angles χ2 (CA-CB-CG-CD1) and χ2 (CA-CB-CG-OD1)) to opti-

**Table 2.** Hydrogen bond interactions between compounds **1**–**4** and residues at the catalytic site of GPb

| Inhibitor atom | GPb-**1** complex | | GPb-**2** complex | | GPb-**3** complex | | GPb-**4** complex | |
|---|---|---|---|---|---|---|---|---|
| | Protein atom | Distance (Å) | Protein atom | Distance (Å) | Protein atom | Distance (Å) | Protein atom | Distance (Å) |
| O2 | Asn284 ND2 | 2.8 | Asn284 ND2 | 3.1 | Asn284 ND2 | 3.1 | Asn284 ND2 | 3.1 |
| | Tyr 573 OH | 2.9 | Tyr 573 OH | 3.1 | Tyr 573 OH | 3.0 | Tyr 573 OH | 3.3 |
| | Glu 672 OE1 | 3.1 | Glu 672 OE1 | 3.1 | Glu 672 OE1 | 3.1 | Glu672 OE1 | 3.3 |
| | Wat96 | 2.8 | Wat131 | 2.8 | Wat100 | 2.8 | Wat92 | 3.0 |
| | Wat335 | 3.1 | Wat304 | 3.3 | Wat223 | 3.2 | Wat218 | 2.8 |
| O3 | Glu672 OE1 | 2.6 | Glu672 OE1 | 2.7 | Glu672 OE1 | 2.7 | Glu672 OE1 | 2.7 |
| | Ser674 N | 3.1 | Ser674 N | 3.1 | Ser674 N | 3.0 | Ser674 N | 3.1 |
| | Gly675 N | 3.1 | Gly675 N | 3.1 | Gly675 N | 3.1 | Gly675 N | 3.1 |
| O4 | Asn484 OD1 | 3.3 | Asn484 OD1 | (3.4) | Gly675 N | 2.7 | Gly675 N | 2.7 |
| | Gly675 N | 2.7 | Gly675 N | 2.7 | Wat131 | 2.9 | Wat123 | 2.6 |
| | Wat126 | 2.9 | Wat130 | 2.9 | | | | |
| O6 | His377 ND1 | 2.7 | His377 ND1 | 2.7 | His377 ND1 | 2.7 | His377 ND1 | 2.7 |
| | Asn484 OD1 | 2.7 | Asn484 OD1 | 2.8 | Asn484 OD1 | 2.8 | Asn484 OD1 | 2.3 |
| O7 | Wat349 | 2.8 | Wat303 | 2.8 | Leu136 N | (3.4) | Leu136 N | 3.0 |
| | | | | | Wat309 | 2.8 | Wat293 | 2.5 |
| O8 | Asn284 N | 2.6 | Asn284 N | 2.9 | Asn284 N | 2.8 | Wat293 | 2.7 |
| | Wat349 | 2.8 | Wat303 | 2.9 | Wat309 | 2.8 | | |
| O9 | Wat351 | 2.7 | | | | | | |
| Total | 17 | | 16 | | 16 | | 15 | |

GPb-**1** complex: Wat96 is hydrogen bonded to Thr671 O, Ala673 N and Wat100. Wat100 is hydrogen bonded to Val379 N, Thr671 O and Wat98. Wat98 is hydrogen bonded to Glu672 O and Wat104. Wat104 is hydrogen bonded to Glu672 O, Gly694 O, and Asp693 OD2. Wat335 is hydrogen bonded to Lys574 NZ, Glu672 OE1, PLP999 O2Pm and Wat58. Wat58 is hydrogen bonded to Gly135 N, Asp283 OD1m and Wat61. Wat61 is hydrogen bonded to Arg569 N and PLP999 O2P. W126 is hydrogen bonded Thr676 OE1 and PLP999 O3P. Wat349 is hydrogen bonded to Asp283 OD1 and Wat79. Wat79 is hydrogen bonded to Gly134 N, Gly137 Nm and Glu88 OE2. Wat351 is hydrogen bonded to His341 NE2.
GPb-**2** complex: Wat131 is hydrogen bonded to Thr688 O, Ala686 N, and Asn804 OD1. Wat304 is hydrogen bonded to Lys574 NZ, Glu672 OE1, PLP999 O2P, and Wat58. Wat58 is hydrogen bonded to Gly135 N, Asp 283 OD1, and Wat63. Wat63 is hydrogen bonded to PLP999 O2P and Arg569 N. Wat130 is hydrogen bonded to Thr676 OE1 and PLP999 O3P. Wat303 is hydrogen bonded to Asp283 OD1 and Wat83. Wat83 is hydrogen bonded to Gly134 N, Gly137 N, and Glu88 OE2.
GPb-**3** complex: Wat100 is hydrogen bonded to Thr671 O, Ala673 N, and Wat105. Wat105 is hydrogen bonded to Val379 N, Thr671 O, and Wat102. W223 is hydrogen bonded to Lys574 NZ, Glu672 OE1, PLP999 O2P, and Wat61. Wat61 is hydrogen bonded to Gly135 N, Asp283 O, and Wat65. Wat65 is hydrogen bonded to PLP999 O2P and Arg569 N. Wat131 is hydrogen bonded to Thr676 OE1 and PLP999 O3P. Wat309 is hydrogen bonded to Asp283 OD1 and Wat83. Wat83 is hydrogen bonded to Gly134 N, Gly137 N, and Glu88 OE2.
GPb-**4** complex: Wat92 is hydrogen bonded to Thr671 O, Ala673 N, and Wat97. Wat97 is hydrogen bonded to Val379 N, Thr671 O, and Wat94. Wat218 is hydrogen bonded to Asp283 OD2, Tyr573 OH, Lys574 NZ, and Wat55. Wat55 is hydrogen bonded to Gly134 N, Asp283 OD1, and Wat58. Wat58 is hydrogen bonded to PLP999 O2P and Arg569 N. Wat123 is hydrogen bonded to PLP999 O3P and Thr676 OE1. **Wat293** is hydrogen bonded to Asp283 OD1 and Wat75. Wat75 is hydrogen bonded to Gly134 N, Gly137 N, and Glu88 OE2.

mize contacts with the ligand. In the GPb-**6** complex, O7 is hydrogen bonded to Wat355, and this in turn is hydrogen bonded to Asn284 N, and to Asn133 ND2, Glu88 OE1, and Asn282 O through another water molecule (Wat106).[31] These two water molecules are displaced by the oxamic acid group in the GPb-**1** complex. Furthermore, Wat335, Wat349 and Wat351 (Wat314, Wat105 and Wat110 in the complex with **6**) shifted by ~1.6, ~2.0 and ~1.1 Å, respectively, to create more space for the oxamic acid group to be accommodated without causing steric hindrance.

The structural comparison between GPb-**1** and GPb-**6** complexes also reveals that the hydrogen bond between N1 and His377 O observed in the GPb-6 complex[20,31] is not retained in the GPb-**1** complex. As a result in the GPb-**6** complex the glucopyranosyl (C1, C2, O2, O4 and O5) and the acetamido (N1, C7, O7 and C8) moieties shift by ~0.4–0.6 Å, and 0.9–1.6 Å, respectively, closer to the His377 (Fig. 4). The inability of compound **1** to form the N1···O His377 hydrogen bond might have an energetic cost, in addition to the loss of energy during desolvation, perhaps explaining the lower affinity of compound **1**.

### 3.2. Compounds 2–4

The methylester of **1**, compound **2**, showed increased affinity ($K_i$ = 0.22 mM) for GPb. The ligand binds to the catalytic site of the enzyme in the same mode as **1**, and with the exception of the water-mediated polar interaction of O9 with His341 NE2, observed in the GPb-**1** complex, it retains the hydrogen bonding interactions of **1** with the protein (Fig. 3b). The structural results show that the $-CH_3$ group (C9) can be accommodated at the catalytic site with essentially no disturbance of the structure by making 2 nonpolar/nonpolar interactions with Leu136 CD1 and CG atoms. In general, compound **2** makes a total of 85 van der Waals interactions (9 nonpolar/nonpolar, 20 polar/polar and 56 polar/nonpolar) (Table 3).

The ethylester of **1**, compound **3**, binds 4 times less tightly than **1**, despite the additional interactions of the $-CH_2CH_3$ group (C9 and C10) with the protein. The pattern of hydrogen bonding interactions, illustrated in Fig. 3c, between the inhibitor and the enzyme is maintained when comparing the complex structures of derivatives **2** and **3**. The positioning of $-CH_2CH_3$ group

is towards His341 of the β-pocket. There are in total 90 van der Waals interactions (11 nonpolar/nonpolar, 22 polar/polar and 57 nonpolar/polar) (Table 2) in the GPb-**3** complex.

In compound **4**, with a *N*′-cyclopropyl oxalamide group and a more rigid geometry (compared to **3**) there are additional interactions with the adjacent residues Asn284, Asp339, and His341 (Fig. 3d). Still, this modification did not result in improved affinity of the derivative ($K_i$ = 1.41 mM); the compound exhibits less favourable binding than compound **3**, whose substituent group has some inherent flexibility.

It is notable that, as in the case of compound **1**, exactly the same conformational rearrangements are observed on binding of **2**–**4** to the catalytic site of GPb. These include small shifts in the side chains of Leu136, Asn282, Asp283, Asn284, Asp339, and Thr378 in order to optimise contacts with ligands. The LSQKAB superposition of the GPb-**1** complex structure with GPb-**2**, GPb-**3**, and GPb-**4** complex structures gave r.m.s. deviations of approximately 0.134, 0.101 and 0.099 Å for Cα atoms, respectively, indicating that the four structures have very similar overall conformations.

In Figure 5, we compare the binding of **1**–**4** and **6** within the catalytic site of GPb. The positions of the glucosyl components of **1**–**4** are similar, while the largest difference (compared to **6**) is in the amide N1 positions, a difference that might reflect the absence of a

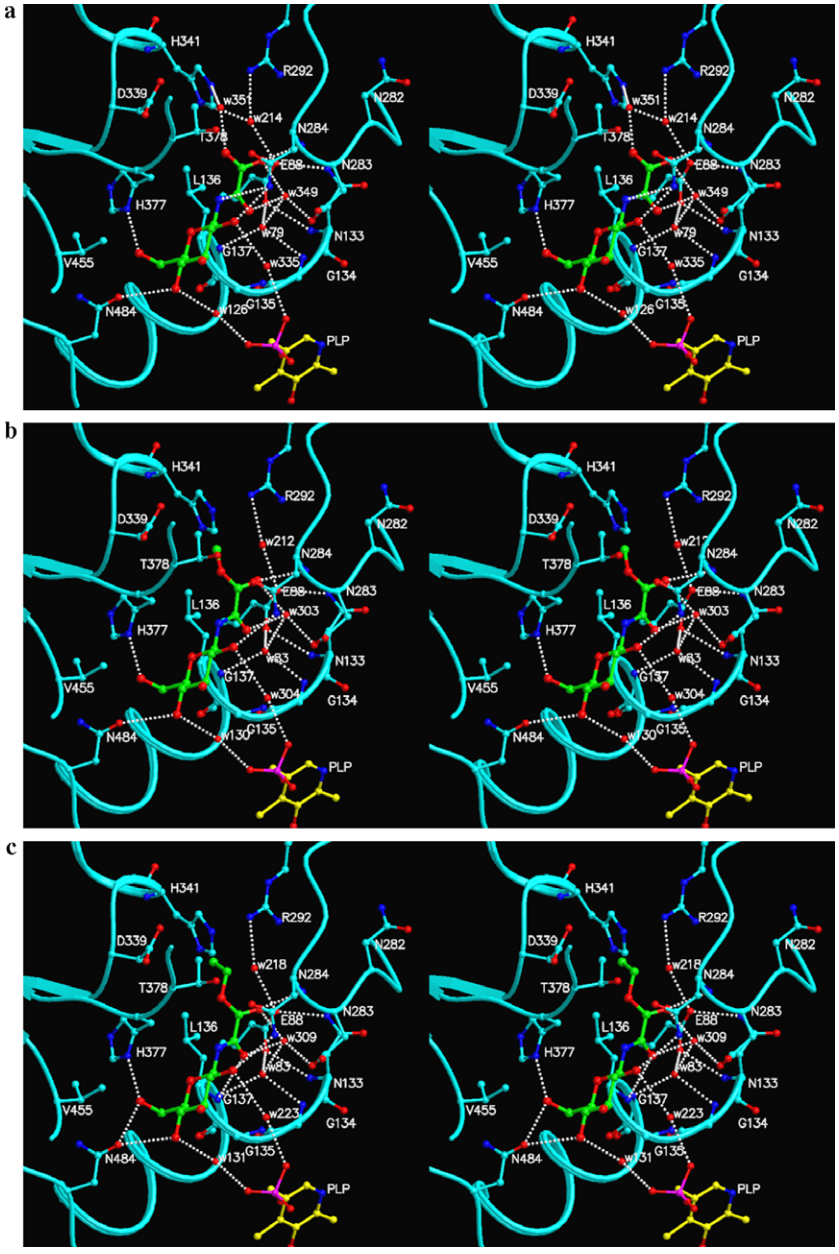


**Figure 3.** Interactions of compounds **1** (a), **2** (b), **3** (c), **4** (d) and **6** (e) with GPb in the vicinity of the catalytic site, shown in stereo. The hydrogen bond pattern between the inhibitors, protein residues and water molecules (w) is represented by dotted lines.

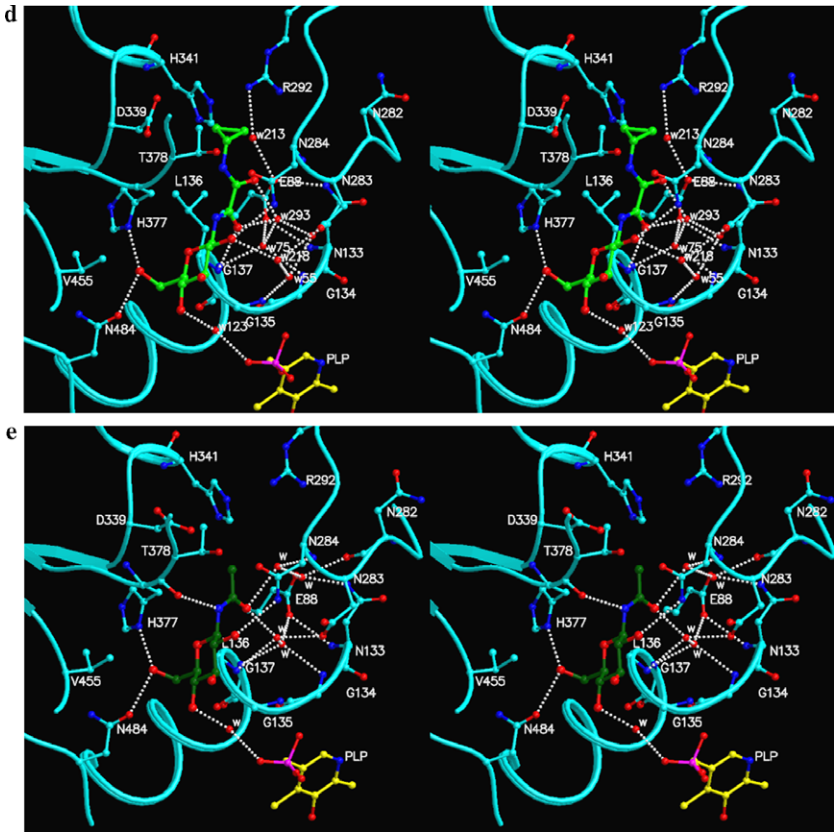


**Figure 3.** (*continued*)

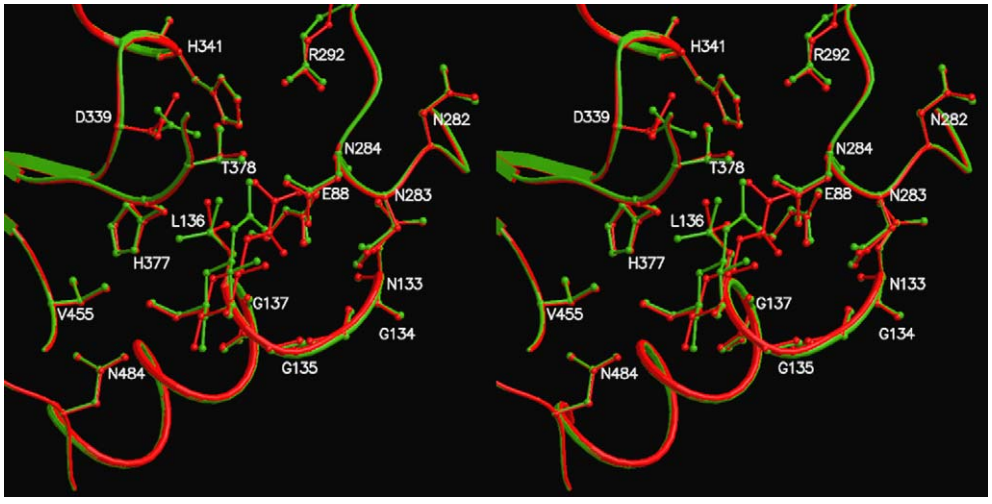


**Figure 4.** Comparison between GPb-**1** complex (orange) and GPb-**6** complex (red) in the vicinity of the catalytic site.

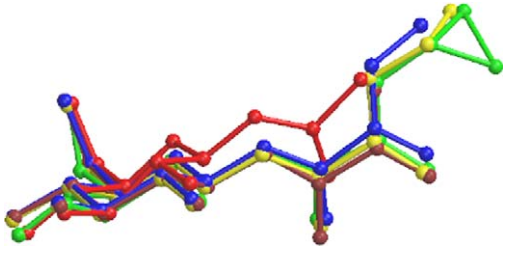

**Figure 5.** Comparison of the positions of the compounds **1** (brown), **2** (blue), **3** (yellow), **4** (green) and **6** (red) bound at the catalytic site of GPb.

hydrogen bond between N1 and main-chain O of His377 in **1**–**4**.

In conclusion, five novel oxalyl derivatives of β-D-glucopyranosylamine, with polar substituents in the amide N1 of the lead compound **6**, were selected for synthesis and crystallographic study. Compounds **1**–**4** are better inhibitors than α-D-glucose but poorer inhibitors than the lead compound **6**, indicating that occupation of the β-pocket results in some unfavourable interactions that are only partially compensated

**Table 3.** Van der Waals interactions between compounds **1**–**4** and residues at the catalytic site of GPb

| Inhibitor atom | GPb-**1** | | GPb-**2** | | GPb-**3** | | GPb-**4** | |
|---|---|---|---|---|---|---|---|---|
| | Protein atom | No. of contacts | Protein atom | No. of contacts | Protein atom | No. of contacts | Protein atom | No. of contacts |
| C1 | Asn284 ND2; His377 O; Wat335 | 3 | His377 O | 1 | His377 O | 1 | Leu136 N; His377 O; Wat218 | 3 |
| C2 | Asn284 ND2; Glu672 OE1; His377 O; Wat96; Wat335 | 5 | His377 O; Glu672 OE1; Wat304; Wat313 | 4 | His377 O; Glu672 OE1; Wat100; Wat223 | 4 | His377 O | 1 |
| O2 | Asn284 OD1,CG | 2 | Asn284 OD1,CG His377 O | 3 | Asn284 OD1,CG; His377 O | 3 | Asn284 OD1,CG; His377 O; | 3 |
| C3 | Glu672 OE1; Gly675 N; Wat126;Wat335 O | 4 | Glu672 OE1; Gly675 N; Wat130; Wat304 | 4 | Glu672 OE1; Gly675 N; Wat131;Wat223 | 4 | Glu672 OE1; Gly675 N; Wat123 | 3 |
| O3 | Glu672 C,CD,CG; Ala673 CA,CB,C,N; Ser674 CA,C; Gly675 CA; Wat96; Wat335 | 12 | Glu672 C,CD,CG; Ala673 CA,CB,C,N; Ser674 CA,C; Gly675 CA; Wat304; Wat313 | 12 | Glu672 C,CD,CG; Ala673 CA,CB,C,N; Ser674 CA,C; Gly675 CA; Wat100; Wat223 | 12 | Glu672 CD,CG ; Ala673 CA,CB,C; Ser674 C; Gly675 CA; Wat92 | 8 |
| C4 | Asn484 OD1; Gly675 N; Wat126 | 3 | Asn484 OD1; Gly675 N; Wat130 | 3 | Asn484 OD1; Gly675 N; Wat131 | 3 | Asn484 OD1; Gly675 N; Wat123 | 3 |
| O4 | Ser674 CA,CB,C,N, OG; Gly675 CA,C,O | 8 | Ser674 CA,CB,C,N; Gly675 CA,C,O; Thr676 CG2 | 8 | Asn 484 OD1; Ser674 CA,CB,C,N,OG; Gly675 CA,C,O; Thr 676 CG2 | 10 | Asn 484 OD1; Ser674 CB,C; Gly675 CA,C,O; Thr 676 N,CG2 | 8 |
| C5 | Gly135 C;Leu136 N; Wat126 | 3 | Gly135 C; Leu136 N; Wat130 | 3 | Gly135 C; Leu136 N; Wat131 | 3 | Gly135 C; Leu136 N; Wat123 | 3 |
| O5 | Leu136 CA,CB,N; His377 CB,ND1 | 5 | Leu136 CA,CB,N ; His377 CB,ND1 | 5 | Leu136 CA,CB,N; His377 CB,ND1 | 5 | Leu136 CA,N; His377 CB,ND1 | 4 |
| C6 | Gly135 C,O; Leu139 CD2; His377 ND1; Asn484 OD1 | 5 | Gly135 C,O; Leu139 CD2; Hi377 ND1; Asn484 OD1 | 5 | Gly135 C,O; Leu139 N,CD2; Hi377 ND1; Asn484 OD1 | 6 | Gly135 C,O; Leu139 CD2; His377 ND1; Asn484 OD1; Wat123 | 6 |
| O6 | Leu139 CD2; His377 CG,CE1; Val455 CB, CG1,CG2; Asn484 CG,ND2 | 8 | Leu139 CD2; His377 CG,CE1; Val455 CB,CG1,CG2; Asn484 CG | 7 | Leu139 CD2; His377 CG,CE1; Val455 CG1,CG2; Asn484 CG | 6 | Leu139 CD2; His377 CG,CE1; Val455 CG1,CG2; Asn284 CG | 6 |
| N1 | Asp284 ND2; His377 CB,O | 3 | Asn284 CG,OD1,ND2; His377 CB,O | 5 | Asn284 OD1,ND2; His377 CB,O | 4 | Asn284 OD1,ND2; His377 CB,O | 4 |
| C7 | Leu136A CB;Asn284 ND2,CG; Wat349 | 4 | Leu136 CB; Asn284 ND2,CG,OD1; Wat303 | 5 | Leu136 CB; Asn284 ND2,CG; Wat309 | 4 | Leu136 N,CB; Asn284 ND2; Wat293 | 4 |
| O7 | Leu136 CB; Leu136 N; Asp283 OD1; Asn284 ND2; Wat58; Wat79 O | 6 | Leu136 N,CB; Asp283 OD1,ND2; Wat58; Wat83 | 6 | Leu136 CA,CB; Asp283 OD1; Asn284 ND2; Wat61; Wat83 | 6 | Leu136 CA,CB; Wat75 | 3 |
| C8 | Asn284 CA,N,ND2, CG,OD1; Wat349; Wat351 | 7 | Asn284 CA,N,ND2,CG,OD1; Wat303 | 6 | Asn284 N,OD1,ND2,CG; Wat309 | 5 | Leu136 CB; Asn284 ND2; Wat293 | 3 |
| O8 | Asp283 CA,C; Asn284 CA,CG, ND2; Wat351 | 6 | Asp283 CG,ND2,OD1; Asn284 CA | 4 | Asp283 C,CG,ND2; Asn284 CA | 4 | Asn284 N | 1 |
| O9 | Leu136 CD1; Asn284 ND2,OD1,CG | 4 | Asn284 OD1 | 1 | Asn284 CG,OD1 | 2 | | |
| N2 | | | | | | | Asn284 OD1 | 1 |
| C9 | | | Leu136 CD1; Asp339 CG,OD2 | 3 | Asn284 CG; Thr378 CG2 | 2 | Thr378 CG2 | 1 |
| C10 | | | | | Leu136 CD1; Asp339 CG,OD1,OD2; His341 CE1,NE2 | 6 | Asn284 CA,N; His341 NE2 | 3 |
| C11 | | | | | | | Asp339 OD1,CG,OD2; His341 CE1,NE2 | 5 |
| Total | | 88 | | 85 | | 90 | | 73 |

by other contacts. All four derivatives form direct and water-mediated hydrogen bonds and extensive van der Waals interactions with residues of the 280s loop (Asp283 and Asn284), the glycine helix (Gly134 and Gly137), Glu88, Asp339 and His341. These interactions provide a rationale for their potency to inhibit GPb activity. In contrast to previously known β-D-glucopyranose analogue inhibitors of GP[20,21,26,30,31] that bind to the catalytic site, compounds **1**–**4** do not exploit the hydrogen bonding interaction between the ligand amide nitrogen and the main-chain carbonyl O of His377. This interaction is an essential feature for the tight binding of compound **6** ($K_i$ = 32 μM), contributing approximately 1.1 kcal/mol to the binding energy with respect to compound **2**. Furthermore, the energy cost for the small conformational changes in the side chain of the amino acid residues and water structure, the increased hydrophilicity, as well as the loss of conformational entropy of the analogues with more flexible side chains (compounds **2**–**4**) on binding might outweigh the gain from the increased interactions. This may explain why lead modification led to decreases in potency. The present study has demonstrated that these novel analogues are competitive inhibitors of the enzyme albeit with moderate affinity. Further work is currently under progress to examine modified analogues with greater potency for the catalytic site of the enzyme.

## Acknowledgements

This work was supported by Greek GSRT through PENED-204/2001, and Scientific and Technological cooperation between Greece and USA (2005-2006), SRS Daresbury Laboratory (Contract No. IHPP HPRI-CT-1999-00012) and the EMBL-Hamburg outstation under FP6 'Structuring the European Research Area Programme' Contract No. RII3/CT/2004/5060008. Synthetic work (TG) was supported from the Greek Ministry of Education (Pythagoras II) and the University of Athens (Special Account). We also wish to acknowledge the assistance of Ms. M. N. Kosmopoulou for help in crystallization experiments.

## References and notes

1. Aiston, S.; Hampson, L.; Gómez-Foix, A. M.; Guinovart, J. J.; Agius, L. *J. Biol. Chem.* **2001**, *276*, 23858.
2. McCormack, J. C.; Westergaard, N.; Kristiansen, M.; Brand, C. L.; Lau, J. *Curr. Pharm. Des.* **2001**, *7*, 1451.
3. Treadway, J. L.; Mendys, P.; Hoover, D. J. *Expert. Opin. Investig. Drugs* **2001**, *10*, 439.
4. Latsis, T.; Andersen, B.; Agius, L. *Biochem. J.* **2002**, *368*, 309.
5. Aiston, S.; Coghlan, M. P.; Agius, L. *Eur. J. Biochem.* **2003**, *270*, 2773.
6. Oikonomakos, N. G. *Curr. Protein Pept. Sci.* **2002**, *3*, 561.
7. Kurukulasuriya, R.; Link, J. T.; Madar, D. J.; Pei, Z.; Richards, S. J.; Rohde, J. J.; Souers, A. J.; Szczepankiewicz, B. G. *Curr. Med. Chem.* **2003**, *10*, 123.
8. Lu, Z.; Bohn, J.; Bergeron, R.; Deng, Q.; Ellsworth, K. P.; Geissler, W. M.; Harris, G.; McCann, P. E.; McKeever, B.; Myers, R. W.; Saperstein, R.; Willoughby, C. A.; Yao, J.; Chapman, K. *Bioorg. Med. Chem. Lett.* **2003**, *13*, 4125.
9. Ogawa, A. K.; Willoughby, C. A.; Bergeron, R.; Ellsworth, K. P.; Geissler, W. M.; Myers, R. W.; Yao, J.; Harris, G.; Chapman, K. T. *Bioorg. Med. Chem. Lett.* **2003**, *13*, 3405.
10. Somsák, L.; Nagy, V.; Hadady, Z.; Docsa, T.; Gergely, P. *Curr. Pharm. Des.* **2003**, *9*, 1177.
11. Kristiansen, M.; Andersen, B.; Iversen, L. F.; Westergaard, N. *J. Med. Chem.* **2004**, *47*, 3537.
12. Klabunde, T.; Wendt, K. U.; Kadereit, D.; Brachvogel, V.; Burger, H.-J.; Herling, A. W.; Oikonomakos, N. G.; Kosmopoulou, M. N.; Schmoll, D.; Sarubbi, E.; von Roedern, E.; Schönafinger, K.; Defossa, E. *J. Med. Chem.* **2005**, *48*, 6178.
13. Oikonomakos, N. G.; Kosmopoulou, M. N.; Chrysina, E. D.; Leonidas, D. D.; Kostas, I. D.; Wendt, K. U.; Klabunde, T.; Defossa, E. *Protein Sci.* **2005**, *14*, 1760–1771.
14. Wright, S. W.; Rath, V. L.; Genereux, P. E.; Hageman, D. L.; Levy, C. B.; McLure, L. D.; McCoid, S. C.; McPherson, R. K.; Schelhorn, T. M.; Wilder, D. E.; Zavadoski, W. J.; Gibbs, E. M.; Treadway, J. L. *Bioorg. Med. Chem. Lett.* **2005**, *15*, 459.
15. Chrysina, E. D.; Kosmopoulou, M. N.; Tiraidis, C.; Kardakaris, R.; Bischler, N.; Leonidas, D. D.; Hadady, Z.; Somsak, L.; Docsa, T.; Gergely, P.; Oikonomakos, N. G. *Protein Sci.* **2005**, *14*, 873.
16. Baker, D. J.; Timmons, J. A.; Greenhalff, P. L. *Diabetes* **2005**, *54*, 2453.
17. Martin, J. L.; Veluraja, K.; Johnson, L. N.; Fleet, G. W. J.; Ramsden, N. G.; Bruce, I.; Oikonomakos, N. G.; Papageorgiou, A. C.; Leonidas, D. D.; Tsitoura, H. S. *Biochemistry* **1991**, *30*, 10101.
18. Watson, K. A.; Mitchell, E. P.; Johnson, L. N.; Son, J. C.; Bichard, C. J. F.; Orchard, M. G.; Fleet, G. W. J.; Oikonomakos, N. G.; Leonidas, D. D.; Kontou, M.; Papageorgiou, A. C. *Biochemistry* **1994**, *33*, 5745.
19. Bichard, C. J. F.; Mitchell, E. P.; Wormald, M. R.; Watson, K. A.; Johnson, L. N.; Zographos, S. E.; Koutra, D. D.; Oikonomakos, N. G.; Fleet, G. W. J. *Tetrahedron Lett.* **1995**, *36*, 2145.
20. Oikonomakos, N. G.; Kontou, M.; Zographos, S. E.; Watson, K. A.; Johnson, L. N.; Bichard, C. J. F.; Fleet, G. W. J.; Acharya, K. R. *Protein Sci.* **1995**, *4*, 2469.
21. Watson, K. A.; Mitchell, E. P.; Johnson, L. N.; Cruciani, G.; Son, J. C.; Bichard, C. J. F.; Fleet, G. W. J.; Oikonomakos, N. G.; Kontou, M.; Zographos, S. E. *Acta Crystallogr.* **1995**, *D51*, 458.
22. Gregoriou, M.; Noble, M. E. M.; Watson, K. A.; Garman, E. F.; Krulle, T. M.; Fuente, C.; Fleet, G. W. J.; Oikonomakos, N. G.; Johnson, L. N. *Protein Sci.* **1998**, *7*, 915.
23. Somsák, L.; Kovács, L.; Tóth, M.; Ősz, E.; Szilágyi, L.; Györgydeák, Z.; Dinya, Z.; Docsa, T.; Tóth, B.; Gergely, P. *J. Med. Chem.* **2001**, *44*, 2843.
24. Oikonomakos, N. G.; Skamnaki, V. T.; Ősz, E.; Szilágyi, L.; Somsák, L.; Docsa, T.; Tóth, B.; Gergely, P. *Bioorg. Med. Chem.* **2002**, *10*, 261.
25. Oikonomakos, N. G.; Kosmopoulou, M.; Zographos, S. E.; Leonidas, D. D.; Chrysina, E. D.; Somsák, L.; Nagy, V.; Praly, J.-P.; Docsa, T.; Tóth, B.; Gergely, P. *Eur. J. Biochem.* **2002**, *269*, 1684.
26. Chrysina, E. D.; Oikonomakos, N. G.; Zographos, S. E.; Kosmopoulou, M. N.; Bischler, N.; Leonidas, D. D.; Kovács, L.; Docsa, T.; Gergely, P.; Somsák, L. *Biocatal. Biotransform.* **2003**, *21*, 233.

27. Györgydeák, Z.; Hadady, Z.; Felföldi, N.; Krakomperger, A.; Nagy, V.; Tóth, M.; Brunyánszki, A.; Docsa, T.; Gergely, P.; Somsák, L. *Bioorg. Med. Chem.* **2004**, *12*, 4861.
28. Archontis, G.; Watson, K. A.; Xie, Q.; Andreou, G.; Chrysina, E. D.; Zographos, S. E.; Oikonomakos, N. G.; Karplus, M. *Proteins* **2005**, *61*, 984.
29. Chrysina, E. D.; Kosmopoulou, M. N.; Kardakaris, R.; Bischler, N.; Leonidas, D. D.; Kannan, T.; Loganathan, D.; Oikonomakos, N. G. *Bioorg. Med. Chem.* **2005**, *13*, 765.
30. Watson, K. A.; Chrysina, E. D.; Tsitsanou, K. E.; Zographos, S. E.; Archontis, G.; Fleet, G. W. J.; Oikonomakos, N. G. *Proteins* **2005**, *61*, 966.
31. Anagnostou, E.; Kosmopoulou, M. N.; Chrysina, E. D.; Leonidas, D. D.; Hadjiloi, T.; Tiraidis, C.; Györgydeák, Z.; Somsák, L.; Docsa, T.; Gergely, P.; Oikonomakos, N. G. *Bioorg. Med. Chem.* **2006**, *14*, 181.
32. Oikonomakos, N. G.; Melpidou, A. E.; Johnson, L. N. *Biochim. Biophys. Acta* **1985**, *832*, 248.
33. Otwinowski, Z.; Minor, W. *Methods Enzymol.* **1997**, *276*, 307.
34. Brünger, A. T.; Adams, P. D.; Clore, G. M.; DeLano, W. L.; Gros, P.; Grosse-Kunstleve, R. W.; Jiang, J.-S.; Kuszewski, J.; Nilges, M.; Pannu, N. S.; Read, R. J.; Rice, L. M.; Simonson, T.; Warren, G. L. *Acta Crystallogr.* **1998**, *D54*, 905.
35. Jones, T. A.; Zou, J. Y.; Cowan, S. W.; Kjeldgaard, M. *Acta Crystallogr.* **1991**, *A47*, 110.
36. Laskowski, R. A.; MacArthur, M. W.; Moss, D. S.; Thornton, J. M. *J. Appl. Crystallogr.* **1993**, *26*, 283.
37. Collaborative Computational Project No 4. Acta Crystallogr. 1994, D50, 760.
38. Luzatti, V. *Acta Crystallogr.* **1952**, *5*, 802.
39. Kraulis, P. *J. Appl. Crystallogr.* **1991**, *24*, 946.
40. Esnouf, R. M. *J. Mol. Graph. Modell.* **1997**, *15*, 132.
41. Merritt, E. A.; Bacon, D. J. *Methods Enzymol.* **1997**, *277*, 505–524.
42. Wen, X.; Sun, H.; Liu, J.; Wu, G.; Zhang, L.; Wu, X.; Ni, P. *Bioorg. Med. Chem. Lett.* **2005**, *15*, 4944.
43. Wen, X.; Zhang, L.; Liu, J.; Zhang, L.; Wu, X.; Ni, P.; Sun, H. *Bioorg. Med. Chem. Lett.* **2006**, *16*, 722.
44. Furukawa, S.; Tsurumi, Y.; Murakami, K.; Nakanishi, T.; Ohsumi, K.; Hashimoto, M.; Nishikawa, M.; Takase, S.; Nakayama, O.; Hino, M. *J. Antibiot. (Tokyo)* **2005**, *58*, 497.
45. Furukawa, S.; Murakami, K.; Nishikawa, M.; Nakayama, O.; Hino, M. *J. Antibiot. (Tokyo)* **2006**, *58*, 503.